Role of minor additions on metallic glasses and composites

Sergio González[a)]
Faculty of Engineering and Environment, Northumbria University, Newcastle upon Tyne NE1 8ST, United Kingdom

(Received 20 June 2015; accepted 2 October 2015)

Microalloying refers to the addition of a small concentration of an alloying element to tune the properties of the parent alloy. Microalloying technology enables to control the glass formation and the mechanical properties of bulk metallic glasses (BMGs). This manuscript presents a comprehensive review on recent developments and breakthroughs in the field of microalloying for tuning the properties of BMGs and composites with focus on the results. The ability of multiple element co-addition to optimize the glass formation and the importance of future alloy developments have been highlighted. Proper microalloying can be used to tailor not only the mechanical properties of the amorphous phase but also those of the crystalline phase, which opens up the possibility for tuning the mechanical performance at different length scales. The effectiveness in controlling the mechanical performance through microalloying was shown to greatly depend on the alloy composition and closeness to the critical amorphous diameter. A tentative outlook commenting the potential and challenges of this exciting field of research is also presented.

Sergio González

Dr. González is a senior lecturer at Northumbria University who joined in December 2014 after working in the University of Manchester as a research associate. Prior to that, he held research positions at the Autonomous University of Barcelona (2011–2013) and at the WPI-AIMR Institute at Tohoku University in Japan (2008–2010). He received a BEng in Mechanical Engineering at the Pontifical Comillas University of Madrid and a BEng in Materials Engineering at the Polytechnic University of Madrid. Afterward, he got his PhD in Materials Physics at Complutense University of Madrid (2004–2008). His PhD research work was carried out at the National Center for Metallurgical Research (CENIM) in Madrid, Spain.

I. INTRODUCTION

Microalloying technology, i.e., usually alloying with <2 at.% alloying elements,[1] has traditionally been used as a metallurgical technique for developing new metallic crystalline materials with improved performance. For example, it can refine the microstructure of steels (adding V, Nb or Ti) and aluminum alloys (adding Zr). It has been recently shown, that minor addition of Sc (0.3 wt%) to bulk ultrafine grained/nanocrystal Al–Cu alloy increases the ductility and strength of the alloy to about 275 and 50%, respectively, compared to that of the alloy without Sc.[2] The prolongation of the ductility was attributed to the promotion of intragranular precipitation of θ'-Al_2Cu nanosized particles. This precipitation has two effects, first, the particles encourage dislocation trapping in the grain interior, and second, they help in accumulating dislocations and sustain work hardening. The work hardening behavior can be also detected in shape memory materials such as those corresponding to the NiTi[3] system or in the ZrCu alloy.[4] However, in shape memory alloys, work-hardening occurs due to the mechanically driven transformation of austenite into a harder phase, martensite.

A relatively new class of material is metallic glass, which is formed when a metallic liquid is cooled fast enough to lead to the formation of a vitreous solid. This material lacks a crystalline lattice and does not exhibit a long-range atomic order but exhibits short to medium range order clusters.[5–7] Since the first metallic glass $Au_{81}Si_{19}$ was obtained by splat quenching in 1960,[8] new compositions have been discovered over the years. The basic idea for metallic glass formation is to suppress the homogeneous nucleation of crystals[9] and to control

Contributing Editor: Jörg F. Löffler
[a)]Address all correspondence to this author.
e-mail: sergio.sanchez@northumbria.ac.uk
DOI: 10.1557/jmr.2015.319

their growth to avoid crystallization. The GFA was reported to be directly linked to the crystal growth rate in the supercooled liquid region.[10] Generally, the crystal growth rate is inversely proportional to the viscosity of the supercooled liquid. As bulk metallic glass (BMG) forming liquids are densely packed, they show high viscosity and sluggish crystallization kinetics when compared with other metallic liquids and they exhibit an intermediate behavior between the strongest and the most fragile liquids. To predict the GFA, many parameters have been used over the years such as the supercooled liquid region $\Delta T_x = T_x - T_g$, the reduced glass transition temperature $T_{rg} = T_g/T_l$ and the γ parameter $[T_x/(T_g + T_l)]$, where T_x is the crystallization temperature, T_g is the glass transition temperature and T_l is the liquidus temperature.[11–13] Additionally, for Ti-based BMGs, the electronic structure (electrons per atom: *e*/a) is an important parameter to predict the GFA.[14]

Metallic glasses exhibit interesting properties, such as high yield strength and low elastic modulus. However, they are generally brittle because they exhibit shear softening, a phenomenon that originates from shear-induced dilatation[15–18] that causes highly localized shear bands and catastrophic failures. Metallic glasses can be ductilized by promoting the multiplication and arrest of shear bands, which can be attained by promoting the formation of crystalline phases by destabilizing the liquid phase through microalloying. The addition of minor alloying elements can affect the stability of the crystalline phase during quenching and thus determine the evolution of the microstructure. For example, in shape memory metallic glass composites it influences the eutectoid decomposition of the high temperature metastable crystalline B2 CuZr phase, which affects the formation and competition among B2 CuZr, the low-temperature equilibrium crystalline phase and the amorphous phase during quenching as reported by Song et al.[19] The shifting in the B2 CuZr phase transformation is significantly influenced by minor element addition because it can significantly change the electronic structure and bonding energies of the B2 phase. The impact of the electronic structure on the stability of the B2 phase can be assessed from the number of valence electrons per atom (e/a). These authors proposed a new strategy for the formation of CuZr-based shape memory BMG composites and suggested a new parameter $K = T_f/T_L$, where T_f and T_L are the final temperature of B2 CuZr phase formation and T_L the liquidus temperature, to predict and select a compositional region for different sized BMGs and composites (BMGC).

The question that arises is that whether the techniques used to tune the mechanical properties of crystalline materials can be applied in metallic glasses. Pauly et al.[20] showed that crystalline particles present in Cu–Zr–(Al–Ti) BMG composites can exhibit martensitic transformation that lead to work hardening and enhanced plastic deformation. The martensitic phase transformation from B2 austenite to B19′ martensite resulted in plastic strains of up to 15%. Similar results are traditionally obtained with fully crystalline shape memory materials, thus confirming the validity of the techniques for BMGs. In fact, Wu et al.[21] found a few years later that promoting twinning of the reinforcing crystals present in BMGs through microalloying can improve the ductility of the BMGC similarly to that detected in microalloyed nanocrystalline materials.[22,23]

Microalloying technology can be also used to tailor the structure of the amorphous phase and thus control the mechanical performance of the material. Microalloying can have different effects on the melt, depending on the composition of the BMG and the nature of the elements added (rare earth element ≡ RE, transition metal ≡ TM, etc). For example, they can change the density of states,[24] stabilize the liquid phase by approaching the composition closer to a deep eutectic,[25] impair the thermodynamic driving force for crystal precipitation by introducing an atomic-level strain energy into the liquid,[26] favor the formation of local crystal-like orders at the atomic scale[27] or scavenge oxygen from the melt.[5] Over the years, the vast majority of the studies have been focused on studying the effect of adding one minor alloying element to tune the GFA and the mechanical properties of BMGs and BMGCs. Only few studies have dealt with the effect that minor co-addition of various elements[28–30] has on the properties of these materials, despite the fact that the synergistic effect of minor element co-addition can result in compositions with very different properties as shown in this paper.

Another issue of interest is the dramatic change in the structure and thus on mechanical performance that microalloying could have in the properties of these materials. This is especially important for BMGs whose structure is very sensitive to compositional changes and for samples with dimensions close to the critical amorphous diameter (D_c) since the amorphous phase can turn crystalline with a small composition change. Although this offers the opportunity to tailor the properties of alloys with high efficiency (i.e., small alloying addition has a large effect on the material structure), it implies a technological challenge for controlling the composition.

In this paper, we summarize the effect of microalloying in the glass forming ability and mechanical properties of alloys that are very sensitive to minor additions with focus on our results. This sensitivity is either because their glass forming ability is relatively low and thus a small composition change can lead to crystallization [i.e., for Mg–Ni–RE,[31] Mg–Zn–Ca,[32] and Al–Ni–Co–Y[33] systems] or because the alloy system itself is very sensitive to minor additions (i.e., for Zr–Cu alloys).[25,34]

II. INFLUENCE ON PROPERTIES

A. Tuning the glass forming ability

1. Addition of RE elements

Due to the affinity of RE elements for oxygen, they can scavenge oxygen impurity and promote the formation of innocuous oxides which results in an increase of the GFA.[4] However, a drawback for using RE elements is that microalloying element is relatively expensive. A cheaper and sometimes more effective option, to increase the GFA, is to use mischmetal (MM), i.e., a mixture of RE elements in naturally occurring proportions. There are several types of MMs such as LaMM (lanthanum mischmetal) and CeMM (cerium mischmetal), which are named according to the most abundant element present in the mixture.

Table I lists the critical amorphous diameter (D_c) of various alloys corresponding to the Mg–Ni–La system and the same alloys when La is fully substituted by LaMM.[31] Among these compositions, the $Mg_{65}Ni_{20}LaMM_{15}$ is the one which exhibits the highest D_c. Also, it is the composition for which the critical amorphous diameter increases the most, from 0.5 to 2 mm, after the substitution of La by LaMM. The GFA parameters ΔT_x, T_{rg}, and γ were calculated from the measured parameters (glass transition temperature: T_g, crystallization onset temperature: T_x, solidus temperature: T_m and liquidus temperature: T_l), however, no clear correlation between D_c and either ΔT_x or T_{rg} was observed. Moreover, the magnitude of the γ parameter is relatively insensitive to compositional changes. These results suggest that the parameters ΔT_x, T_{rg}, and γ are not reliable indicators of the GFA for this set of alloys.[31]

To understand the reason for the high GFA of the $Mg_{65}Ni_{20}LaMM_{15}$ alloy, the ratio of Mg:Ni:REs was held constant at 65:20:15, as the original alloy. Table II shows the value of D_c for alloys with the same proportion of RE elements as in the LaMM.[31] The value of D_c increases with increasing content of Nd, which is consistent with the results of Lu et al.[35] These results thus confirm the important role of the Nd content in the glass forming ability. However, small addition of Ce also appears to be beneficial in increasing the D_c. This behavior cannot be explained from differences in heat of mixing the RE elements with Mg since they are very similar: Mg–La (−7 KJ/mol), Mg–Ce (−7 KJ/mol), Mg–Pr (−6 KJ/mol), and Mg–Nd (−6 KJ/mol).[36] It can neither be explained from the point of view of differences in atomic radii since they are practically the same for La (0.195 nm), Ce (0.185 nm), Pr (0.185 nm) and Nd (0.182 nm).[37] Li et al.[28] studied the influence of RE elements on the GFA of $Mg_{65}Ni_{20}La_{9.29}Nd_{5.71}$ alloy and observed that when La and Nd atoms were partially replaced by Ce atoms, the GFA increased due to a decrease in the Gibbs free energy of mixing. This phenomenon could also explain the beneficial effect of the Ce addition in enhancing the D_c for $Mg_{65}Ni_{20}La_{8.91}Nd_{5.45}Ce_{0.59}$ alloy.[32] These results suggest that when microalloying elements coexist in a proper ratio in the MM, the mixture can be useful to substitute expensive RE elements, such as La,[38] to increase the GFA of metallic glasses at a relatively low cost. Similar effectiveness in changing the GFA of alloys corresponding to the Mg–Ni–La system is observed when minor Si–La, Y–Si–La and B–La elements are co-added.[39] Minor element co-addition has thus great potential for tuning the GFA of metallic glasses.

The main drawback for using the MM is the lack of an exact formulation, i.e., the composition depends on the location from where the ore is extracted. Differences in composition of the MM could have different effects on the GFA of the alloy and lead to the formation of crystalline phases of different natures, which in turn results in alloys with very different mechanical performances.[40] This limitation makes it impractical to implement the use of the MM by industries. Moreover, the MM contains naturally present impurities coming from the ore that could have a negative effect on the GFA. An efficient technique to better control the final properties of BMGs at a relatively lower cost than using La is the addition of Yttrium (Y). This explains the wide use of this element in controlling the properties of BMGs. The main interest for using Y to increase the GFA generally stems from its effectiveness in scavenging oxygen. However, Wang et al.[27] reported recently that the mechanism for increasing the GFA of the Cu–Zr–Al

TABLE I. Critical amorphous diameter (D_c) for the Mg–Ni–La and Mg–Ni–LaMM systems.[20]

Alloy	D_c (mm)
$Mg_{65}Ni_{20}La_{15}$	0.5
$Mg_{65}Ni_{20}LaMM_{15}$	2
$Mg_{70}Ni_{20}La_{10}$	0.4
$Mg_{70}Ni_{20}LaMM_{10}$	0.5
$Mg_{71}Ni_{18}La_{11}$	0.5
$Mg_{71}Ni_{18}LaMM_{11}$	1
$Mg_{69}Ni_{18}La_{13}$	0.5
$Mg_{69}Ni_{18}LaMM_{13}$	1

TABLE II. Critical amorphous diameter of alloys containing 15 at% RE with the same proportion of RE elements as in the LaMM.[20]

Alloy	D_c (mm)
$Mg_{65}Ni_{20}Nd_{15}$	3.5
$Mg_{65}Ni_{20}La_5Nd_{10}$	2.5
$Mg_{65}Ni_{20}La_{9.29}Nd_{5.71}$	1
$Mg_{65}Ni_{20}La_{8.91}Nd_{5.45}Ce_{0.59}$	2
$Mg_{65}Ni_{20}La_{8.38}Nd_{5.17}Pr_{0.89}Ce_{0.56}$	2
$Mg_{65}Ni_{20}La_{14.06}Ce_{0.94}$	<1

alloy system when 2 at.% Y is added can be attributed to the formation of the local crystal-like orders at the atomic scale. In principle, one could expect that an increase in the crystal-like order should accelerate the crystallization rate of the glass-forming liquid; however, the GFA of the alloy increases. This paradox was explained based on the previous investigation of Cheng et al.[41] where the authors identified the co-existence in the Cu–Zr based BMG of a competition process of the crystal growth and formation of icosahedra-like orders. These icosahedra-like clusters can pin the boundaries of crystal-like clusters and limit their growth,[26] thus resulting in an overall structural ordering that reduces the thermodynamic driving force for crystallization. This process slows down the crystallization rate and thus enhances the GFA.

2. Addition of transition elements

Microalloying with most transition metals can improve the GFA of Al-based BMGs. For example, partial substitution of Al by 0.5 at.% TM (with the exception of the late transition elements Ni and Cu) in the $Al_{88}Y_7Fe_5$ alloy increases the GFA.[42] Among these elements, the early TM elements (Ti, V, and Cr) exhibit larger ΔT_x, from 34 to 44 °C, than the mid TM elements (Co and Fe), ΔT_x from 22 to 27 °C, which is consistent with the larger GFA of the former elements. From synchroton diffraction and EXAFS, it was concluded that the GFA increase with minor Ti addition was due to the formation of short- and medium-range orders that decrease the atomic mobility in the glass, enhancing the glass stability (i.e., increasing the nucleation barrier) and thus making the nucleation of α-Al more difficult.

In other alloy systems the superior GFA is attributed to a covalent atomic interaction. For example, it was observed in Ce–Al–Cu BMGs that addition of 0.2–3.0 at.% of Fe, Co Ni, Nb, Si, C or B increases the maximum amorphous diameter from 2 to 10 mm (Ref. 43) due to the strong covalent interaction between Fe, Co, Ni, Nb, and the Al matrix. Chathoth et al.[44] detected, for the same Ce–Al–Cu alloy system, strong variations in the relaxational dynamics while microalloying with 1 at.% Nb and the enhancement of GFA was correlated with a decrease of the self-diffusivity close to the melting temperature by about 74% and also to a temperature dependence change from Arrhenius to non-Arrhenius behavior.[44] However, TMs can also have a negative effect on the GFA of some systems. Partial substitution of Ni by 3–5 at.% Pd decreases the GFA of the $Zr_{55}Al_{10}Cu_{30}Ni_{(5-x)}Pd_x$ alloy.[45] Addition of Pd promotes the formation of Zr–Pd and Zr–Al pairs that can form Zr–Pd and Zr–Al clusters acting as homogeneous nucleation sites for the Zr_2(Pd, Ni)-type phase and the Zr_3Al_2-type phase, respectively. This is consistent with the decrease of the supercooled liquid region ΔT_x from 82 K for $Zr_{55}Al_{10}Cu_{30}Ni_5$ to 77 K for $Zr_{55}Al_{10}Cu_{30}Pd_5$ alloy. A decrease in the GFA was also observed in the Zr–Cu–Al system with the addition of TM elements, such as Co and Fe, as can be deduced from the diffraction patterns of Fig. 1. For $Zr_{48}Cu_{48}Al_4$ alloy, the GFA decreases when Cu is partly substituted by up to 1 at.% Co.[46] This effect is more remarkable with the addition of Fe since only 0.5 at.% is enough to dramatically decrease the volume fraction of the amorphous phase. The predicted heats of mixing are −41 kJ/mol for Co–Zr, +6 kJ/mol for Co–Cu, −19 kJ/mol for Co–Al, −25 kJ/mol for Fe–Zr, +13 kJ/mol for Fe–Cu and −11 kJ/mol for Fe–Al pair.[35] Consequently, the atomic bondings with Co are stronger than with Fe, which can explain the lower GFA with the addition of Fe. Partial substitution of Cu by Co also decreases the GFA of the Zr–Cu system as observed by Javid et al.[47,48] These authors observed that Co shifts the temperatures of the eutectoid reaction, $CuZr \leftrightarrow Cu_{10}Zr_7 + CuZr_2$, to lower values and thus, increases the thermal stability of the B2 ZrCu phase.

Depending on the transition element added and composition of the alloy, the effect on the GFA may be different. For $Zr_{66.7-x}Ni_{33.3}Pd_x$ alloys, partial substitution of Zr by 1 and 3 at.% Pd (a late TM) enhances the GFA and the activation energy for crystallization[49] due to the increase of topological short-range order. Similar GFA increase is observed in $Ni_{57}Zr_{20}Ti_{23-x}Pd_x$ alloys when Ti is partly substituted by 3, 5, 7, and 10 at.% Pd.[50] The addition of Pd to $Ni_{57}Zr_{20}Ti_{23}$ alloy suppresses the formation of the primary cubic Ni(Ti,Zr) phase and increases the GFA. According to Inoue[51] the supercooled liquid state is stabilized when multicomponent systems have large negative heat of mixing. The large negative heat of mixing of Pd–Zr (−91 kJ/mol) and Pd–Ti (−65 kJ/mol)[36] may explain the suppression of Ni(Ti,Zr) phase formation.

Metallic glasses corresponding to the Al–Y–Ni–Co–Pd system, exhibit a decrease in the GFA with the addition of Pd and leads to the formation of different crystalline phases depending on the concentration of the alloying element. For $Al_{85}Y_{8-x}Ni_5Co_2Pd_x$ ribbon samples, a broad diffraction peak was observed for $Al_{85}Y_8Ni_5Co_2$ alloy and the peak tends to form two shoulders with increasing addition of Pd up to 4 at.%,[33] suggesting a decrease in the GFA. Similarly, for 1 mm diameter rods of $Al_{86}Ni_6Y_{6-x}Co_2Pd_x$, partial substitution of Y by 0.5 and 1 at.% Pd results in a dramatic decrease of the GFA,[52] as can be deduced from the diffraction patterns of Fig. 2. For $Al_{86}Ni_6Y_6Co_2$ alloy, peaks corresponding to α-Al and Al_3Ni are superimposed on a broad halo, suggesting the presence of an amorphous or nanocrystalline matrix. For $Al_{86}Ni_6Y_{5.5}Co_2Pd_{0.5}$ and $Al_{86}Ni_6Y_5Co_2Pd_1$ alloys, additional peaks corresponding to Al_9Co_2 and Al_3Y are detected while the broad halo is practically nonexistent. This re-

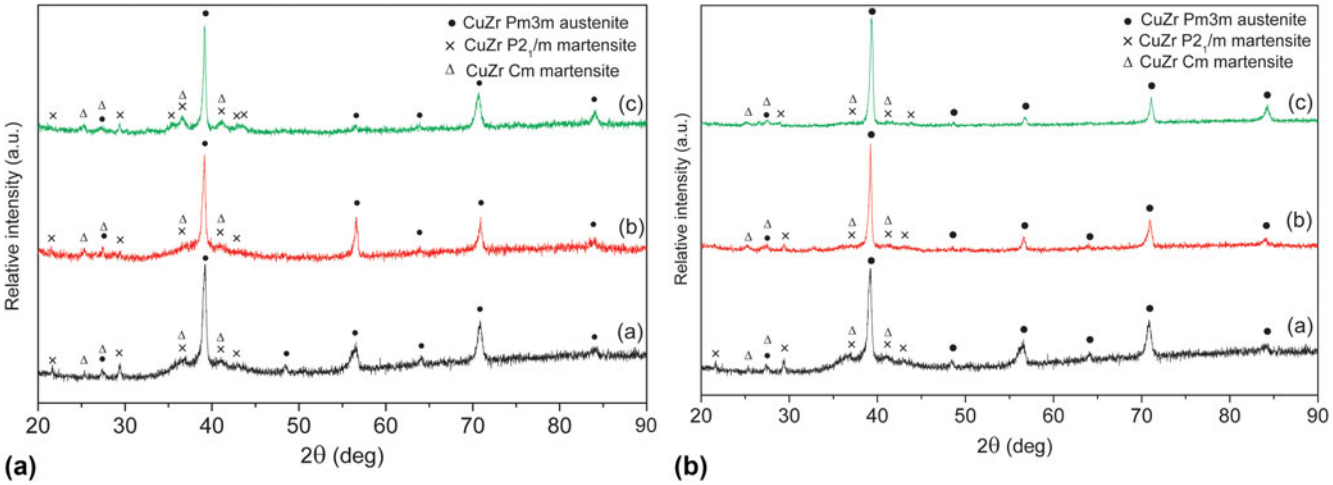

FIG. 1. A) Diffraction patterns corresponding to (a) $Zr_{48}Cu_{48}Al_4$, (b) $Zr_{48}Cu_{47.5}Al_4Co_{0.5}$, and (c) $Zr_{48}Cu_{47}Al_4Co_1$ as-cast rods. B) Diffraction patterns corresponding to (a) $Zr_{48}Cu_{48}Al_4$, (b) $Zr_{48}Cu_{47.5}Al_4Fe_{0.5}$, and (c) $Zr_{48}Cu_{47}Al_4Fe_1$ as-cast rods. (color online)

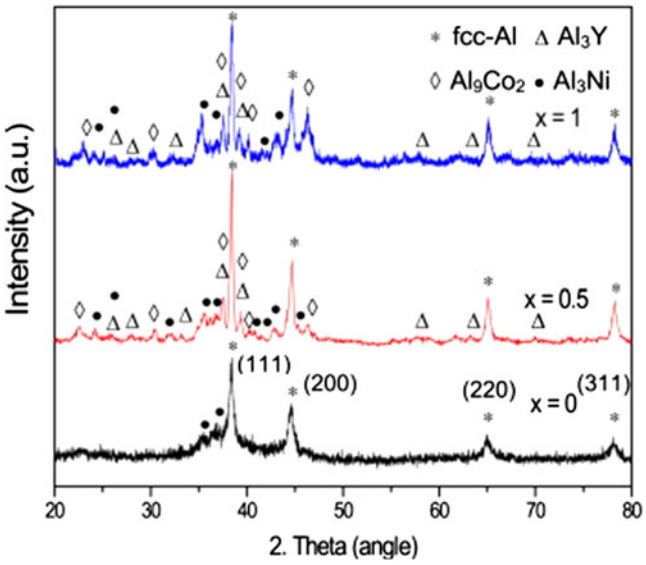

FIG. 2. Diffraction patterns of 1 mm diameter $Al_{86}Ni_6Y_{6-x}Co_2Pd_x$ (x = 0, 0.5 and 1) rods. (color online)

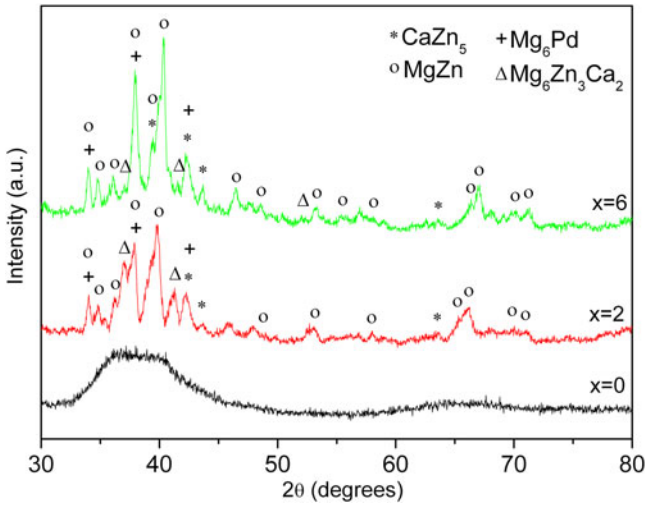

FIG. 3. Diffraction patterns of the as-cast $Mg_{72-x}Zn_{23}Ca_5Pd_x$ (x = 0, 2 and 6) rods. (color online)

duction of the GFA could be explained considering the high binding potential of the Pd–Y pair (i.e., −84 kJ/mol) compared to the relatively low binding potential of the Co–Y (−1 kJ/mol) and Ni–Y (0 kJ/mol) pairs,[36] which would lead to a dramatic driving force for nucleation from Pd–Y pair sites. However, the promotion of α-Al phase formation with Pd addition cannot be explained from the heats of mixing due to the strength of the attractive interaction of the Al–Pd atomic pair. The small atomic size difference between Al and Pd does not favor the atomic packing, which may explain why the GFA decreases.[33]

The addition of Pd to $Mg_{72}Zn_{23}Ca_5$ alloy also decreases the GFA,[53] as can be deduced from the diffraction patterns in Fig. 3. For the alloy without Pd, a broad halo centered at around 39° and a broad peak at about 37° are detected . The results suggest that the alloy consists of an amorphous matrix and nanocrystals embedded in it. However, for $Mg_{70}Zn_{23}Ca_5Pd_2$ and $Mg_{66}Zn_{23}Ca_5Pd_6$ alloys, narrow reflections are present, suggesting the development of a fully crystalline structure. These diffraction patterns are assigned to $CaZn_5$ MgZn, Mg_6Pd, and $Mg_6Ca_2Zn_3$ phases. From the relative change in intensity of the diffraction peaks with increasing content of Pd, it can be deduced that the volume fraction of the different phases change with the alloy composition. The backscattered SEM image in Fig. 4 shows the microstructure of the 3 samples of different compositions. For $Mg_{72}Zn_{23}Ca_5$ alloy, a rather featureless contrast is observed, which is consistent with the diffraction result. However, the microstructures for $Mg_{70}Zn_{23}Ca_5Pd_2$ and

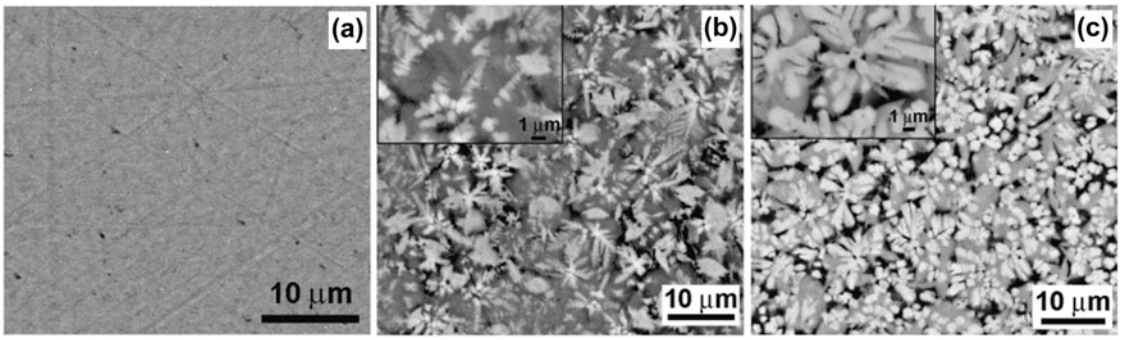

FIG. 4. SEM images (backscattered electrons) of (a) $Mg_{72}Zn_{23}Ca_5$, (b) $Mg_{70}Zn_{23}Ca_5Pd_2$, and (c) $Mg_{66}Zn_{23}Ca_5Pd_6$ rod. The insets show the magnified details of the microstructure of the $Mg_{70}Zn_{23}Ca_5Pd_2$ and $Mg_{66}Zn_{23}Ca_5Pd_6$ samples (in panels (b) and (c)).

$Mg_{66}Zn_{23}Ca_5Pd_6$ alloys are completely different. The microstructures are crystalline and consist of a large volume fraction of dendrites. The dendrites correspond to Mg_6Pd, the gray regions to $CaZn_5$, the black regions to MgZn and the $Mg_6Zn_3Ca_2$ phase corresponds to the areas of darkest tonality that lie within the dark regions associated MgZn. The mechanism responsible for the GFA decrease with Pd addition in this system should be different from that of the $Al_{86}Ni_6Y_6Co_2$ alloy since the binding potential of the alloying element with the other elements of the alloy are relatively similar [i.e., Pd–Mg (−40 kJ/mol), Pd–Zn (−33 kJ/mol) and Pd–Ca (−63 kJ/mol)].[36] The formation of Mg_6Pd probably comes from partial crystallization of the Pd–Mg atomic clusters upon cooling since Mg_6Pd is the first crystalline phase detected in the Mg–Pd system.[54] The heat of mixing of Mg_6Pd (−21 kJ/mol) is larger than that of MgZn (−4 kJ/mol),[55] thus the formation of Mg_6Pd is more thermodynamically favored than the formation of MgZn. However, due to the high concentration of Zn atoms in the alloy, they have high probability to be surrounded by Mg atoms, which can lead to the formation of the intermetallic MgZn. As Pd enters the alloy in the substitution of Mg, the quantity of Mg_6Pd phase that is formed increases, which brings about a decrease in the amount of Mg available to constitute the $Mg_6Ca_2Zn_3$ phase.

B. Effect on the mechanical properties

1. BMGs

The minor addition of elements is very helpful to tune the mechanical properties of BMGs, such as the strength, ductility, toughness, etc. These properties can change, despite a small compositional change might not be enough to change the electronic structure or chemistry of the glass-forming liquid.[56] Garret et al.[56] studied the effect that small additions of Si and Sn has on the toughness of $Cu_{47}Ti_{34}Zr_{11}Ni_8$ BMG. For the three compositions studied, $Cu_{47}Ti_{34}Zr_{11}Ni_8$, $Cu_{47}Ti_{33}Zr_{11}Ni_8Si_1$, and $Cu_{47}Ti_{33}Zr_{11}Ni_8Si_1Sn_2$, they observed a decrease in toughness with increasing content in the alloying element. This behavior was attributed to an increase in the shear modulus (G), yield strength (σ_y), and glass transition temperature (T_g) and a decrease in Poisson's ratio (υ). The minor shifts of the elastic constants (G and υ) with small composition change suggest atomic structural arrangements that have an effect on the fracture behavior. For the most highly alloyed composition, i.e., $Cu_{47}Ti_{33}Zr_{11}Ni_8Si_1Sn_2$, cominor alloying with Si and Sn does not appear to have a synergistic effect on the fracture toughness (although the issue of co-addition was not dealt in the manuscript) since the effect on the of G, σ_y, T_g, and υ values could be expected considering that the concentration of minor elements in $Cu_{47}Ti_{33}Zr_{11}Ni_8Si_1Sn_2$ is 3 times higher than those in $Cu_{47}Ti_{33}Zr_{11}Ni_8Si_1$ alloy.

The toughness of the Zr–Cu–Al BMG system was studied by He et al.[57] for different concentrations of Zr and Al. The atomic structure of the Zr–Cu–Al BMG system consists of rigid icosahedral clusters in different volume fractions depending on the Zr and Al content of the alloy. According to these authors, higher toughness is expected for compositions with high Zr-content since the internal structure contains a lower fraction of the rigid icosahedral clusters. They also suggested to avoid the addition to the Zr–Cu–Al system of TM elements with the high-lying partially-filled d band and strong orbital hybridization with Al since it would be detrimental to toughness. Substitution of Cu with Ni/Co enhances the degree of covalency, and thus decreases the toughness, because these elements elevate the TM-d band which interacts more strongly with the *sp* valence electrons of Al.[57] Recent studies report that microalloying binary Zr–Cu alloys with Al is related to the changes in the cluster's composition, which results in considerable deviation from the random mixing behavior[58] due to the strongly attractive interaction between Al and Zr atoms.[59] The late transition element Ni was also reported to decrease the toughness of Zr–Ti–Be–LTM BMGs.[60] Similarly, minor addition of Fe (0.5 at.%) into Vitreloy 1 ($Zr_{41.2}Ti_{13.8}Cu_{12.5}Ni_{10}Be_{22.5}$) results in the degradation

in fracture toughness from 48.5 to 25 MPa $m^{1/2}$. This phenomenon was associated with the variation in free volume distribution in the glass with minor Fe addition.

Minor alloying addition can also have a dramatic effect on the thermoplastic behavior of BMGs. For example, minor addition of RE elements has a significant effect on the performance of the Zr–Cu–Ni–Al system. The thermoplastic formability of $(Zr_{65}Cu_{17.5}Ni_{10}Al_{7.5})_{100-x}RE_x$ (x = 0.25–3.25 at.%, RE: Y, Gd, Tb, Dy, Ho, Er, Tm, Yb, and Lu) BMGs, was studied by analyzing the relative length shrinkage parameter ($\Delta L/L_0$),[61] which is related with the malleability. The value of the parameter $\Delta L/L_0$ tends to increase with increasing content in the alloying element but the above certain concentration drops dramatically. Among all the RE elements investigated, maximum $\Delta L/L_0$ is attained with the addition of a critical concentration of 2 at.% Er and it drops with further addition of the alloying element. This critical concentration, however, varies with the type of element added. When Y is added, the maximum $\Delta L/L_0$ is reached for a concentration of about 1.2 at.%. The variation in the thermoplastic formability was attributed to the different abilities of RE elements to scavenge oxygen, a phenomenon that has a direct effect on the supercooled liquid region interval.

For certain BMG systems with low GFA, the addition of RE elements can result in partial crystallization of the material and lead to a significant change in the mechanical performance. Partial substitution of Mg by 1 at.% Y in the $Mg_{69}Zn_{27}Ca_4$ alloy is enough to partly crystallize a rod sample of 1 mm diameter and increase the strength from 550 to 1012 MPa.[62] This behavior was attributed to the formation of the crystalline phases $Mg_{12}YZn$ and $Ca_2Mg_6Zn_3$. However, addition of Y to $Cu_{45}Zr_{48}Al_7$ BMG improves the GFA and decreases the compressive fracture strength from 1892 MPa for $Cu_{45}Zr_{48}Al_7$ to 1465 MPa for $Cu_{46}Zr_{48}Al_7Y_5$ due to the reduction in the binding energy.[63]

2. Metallic glass composites

The effect of transition elements on the mechanical performance of alloys depends not only on the type of element (early, middle and late TM) added but also on the composition of the alloy. For example, partial substitution of Zr by Nb does not have a significant change in the mechanical properties of $Zr_{(46-x)}Nb_xCu_{37.6}Ag_{8.4}Al_8$ alloys.[64] Other transition elements such as Co and Fe seem to have a larger influence on the mechanical behavior of BMG composites corresponding to the Zr–Cu–Al system. For CuZr-based metallic glass composites, the second-phase particles consist of B2-CuZr phase that transforms into B19′ martensite upon loading.[65] This transformation, which occurs through twinning,[65,66] leads to overall work hardening and thus enhances the plasticity of the BMG. Larger values of plasticity can be attained when the twinning propensity of the particles upon loading is favored. Wu et al.[21] found that the capability of the B2-CuZr phase for deformation twinning could be tailored through microalloying with transition metals since they allow the tuning of the stacking fault energy of the primary slip system of B2-CuZr phase. The purpose of microalloying is to reduce the stacking fault energy of the primary slip system of reinforcing crystals to improve the twinning propensity thus favoring the martensitic transformation.

The stacking fault energy of base B2-CuZr phase (i.e., 381 mJ/m^2) decreases when half of Cu on the (011) [100] slip plane is replaced by Cr, Fe, Co, Ni, and Ag. Among these elements, the maximum decrease of the stacking fault energy to 75 mJ/m^2 is obtained with Co addition. This substitution promotes martensitic transformation of the crystalline phase and favors work-hardening during the test which contributes to delay necking of the BMG composite.[21]

Another interesting element for microalloying is Fe since it not only is useful for decreasing the stacking fault energy of B2-CuZr but also is cost-effective. To further understand the influence of Co and Fe addition and their concentration on the mechanical properties of the Zr–Cu–Al system, the mechanical properties of $Zr_{48}Cu_{48-x}Al_4M_x$ (M ≡ Co or Fe, x = 0, 0.5, 1 at.%) BMG composites were studied.[46] Figure 5 shows the compressive stress–strain curves of the $Zr_{48}Cu_{48}Al_4$, $Zr_{48}Cu_{47.5}Al_4Co_{0.5}$, $Zr_{48}Cu_{47}Al_4Co_1$, $Zr_{48}Cu_{47.5}Al_4Fe_{0.5}$ and $Zr_{48}Cu_{47}Al_4Fe_1$ as-cast rods. From these results, it can be deduced that microalloying not only has an influence on the plastic deformation but also on the yield stress. The maximum compressive plasticity of 6.2% is

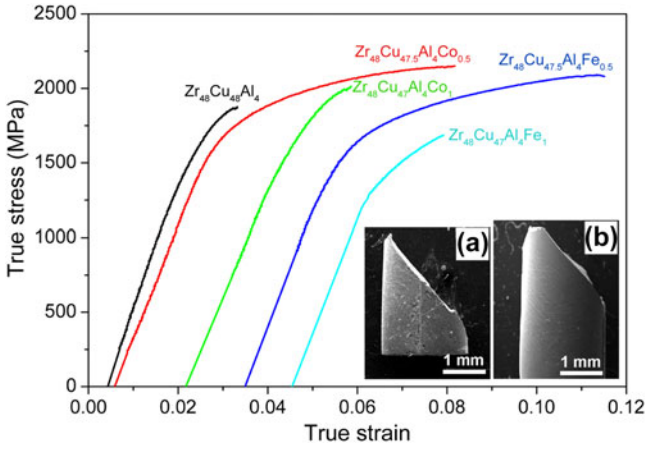

FIG. 5. Compressive stress–strain curves of the $Zr_{48}Cu_{48}Al_4$, $Zr_{48}Cu_{47.5}Al_4Co_{0.5}$, $Zr_{48}Cu_{47}Al_4Co_1$, $Zr_{48}Cu_{47.5}Al_4Fe_{0.5}$, and $Zr_{48}Cu_{47}Al_4Fe_1$ as-cast rods. The insets are optical micrographs showing the fracture angle for (a) $Zr_{48}Cu_{47.5}Al_4Co_{0.5}$ and (b) $Zr_{48}Cu_{47.5}Al_4Fe_{0.5}$ rods. The compression curves have been shifted horizontally for the sake of clarity. (color online)

attained for 0.5 at.% Fe. However, the yield stress decreases gradually from 1390 MPa (for 0.5 at.% Fe) to 1355 MPa (for 1 at.% Fe) with increasing content of Fe. The change in the plastic deformation and yield stress is due to the propensity for the mechanically-driven martensitic transformation of the pristine austenite phase. Other factors such as the co-existence of the amorphous and crystalline counterparts, the nature of the crystalline phase in the as-cast condition (i.e., austenite or martensite), the volume fraction of crystalline (B2) phase and the tendency for deformation-induced nanocrystallization inside shear bands play an important role in the mechanical performance of these alloys.

To further confirm the role of the stress-induced martensitic transformation on the mechanical performance, all the as-cast samples of the same composition were compressed to 2100 MPa for 4 min, i.e., under similar conditions in the compression test. The occurrence of the deformation-induced martensitic transformation and intragranular nanotwinning was evidenced from TEM (Fig. 6). The SAED pattern [Fig. 6(b)] of various crystallites reveals the coexistence of austenite B2 and martensite B19′ phases. Several intragranular nanotwins are generated inside many of the crystals [Figs. 6(a), 6(c), and 6(d)]. These nanotwins can hinder dislocation motion through the twin boundaries resulting in a hardness increase by the dislocation pile-up mechanism similar to that observed at grain boundaries.[67]

For aluminum alloys corresponding to the Al–Ni–Y–Co system, the addition of Pd was reported to be an effective transition element to control the microstructure and thus the mechanical performance of these alloys. Figure 7 shows the load–displacement (P–h) curves of $Al_{86}Ni_6Y_6Co_2$, $Al_{86}Ni_6Y_{5.5}Co_2Pd_{0.5}$, and $Al_{86}Ni_6Y_5Co_2Pd_1$ alloys with a maximum applied force of 300 mN. This load is high enough to get information from all the phases composing the microstructure and thus it provides a representative average value. The mechanical properties were evaluated measuring the hardness (H), reduced elastic modulus (E_r), ratio $U_{plastic}/U_{total}$, and maximum nanoindentation depth (h_{max}) as shown in the table associated to Fig. 7. Among the three compositions, the softest alloy is the $Al_{86}Ni_6Y_{5.5}Co_2Pd_{0.5}$ because it exhibits the lowest H and largest h_{max}. However, the

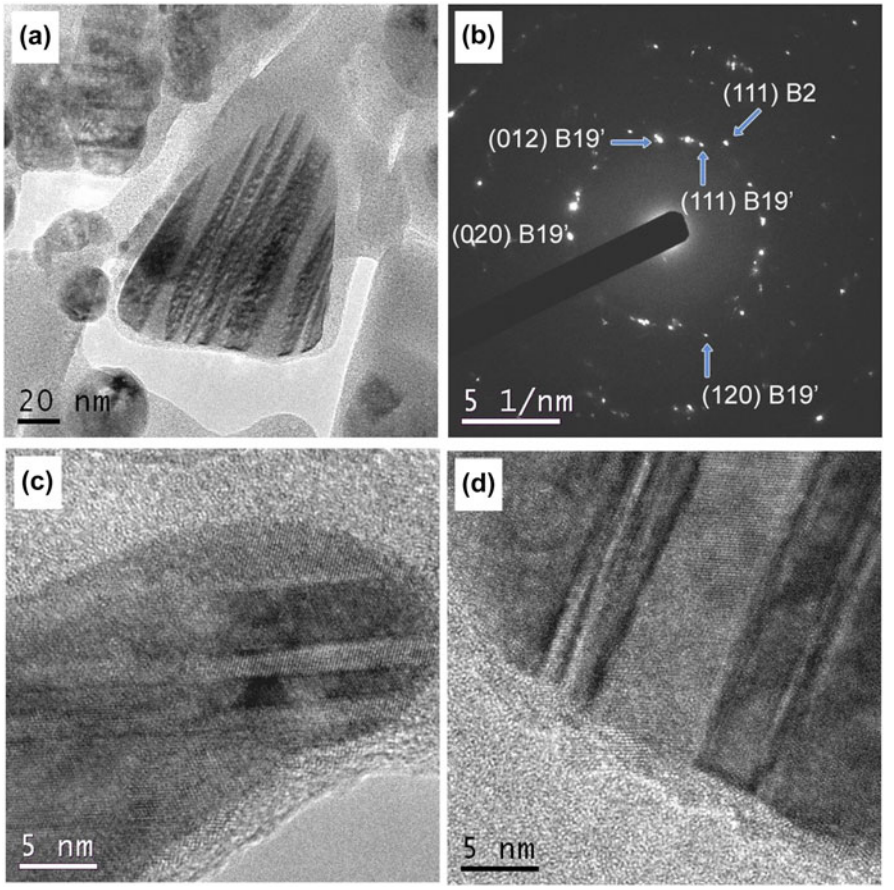

FIG. 6. TEM images of the $Zr_{48}Cu_{47.5}Al_4Fe_{0.5}$ alloy compressed to 2100 MPa for 4 min. Panels (a), (c), and (d) show examples of intragranular nanotwins formed inside the crystalline particles during compression. Panel (b) is a SAED pattern of these crystals, revealing the coexistence of B2 (austenite) and B19′ (martensite) phases. (color online)

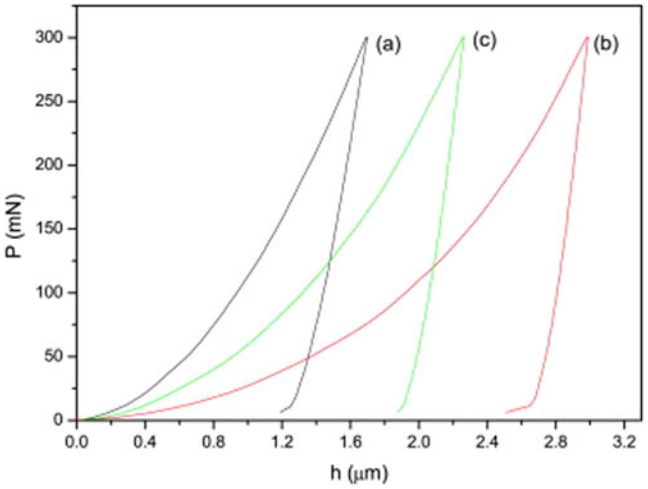

	(a)	(b)	(c)
H (GPa)	5.5	2.5	3
E_r (GPa)	98	88	91
Uplastic/Utotal	0.66	0.78	0.76
h_{max} (μm)	1.7	3	2.3

FIG. 7. *P–h* curves of (a) $Al_{86}Ni_6Y_6Co_2$, (b) $Al_{86}Ni_6Y_{5.5}Co_2Pd_{0.5}$, and (c) $Al_{86}Ni_6Y_5Co_2Pd_1$. The corresponding table lists the hardness (H), reduced elastic modulus (E_r), ratio $U_{plastic}/U_{total}$ and maximum nanoindentation depth (h_{max}). (color online)

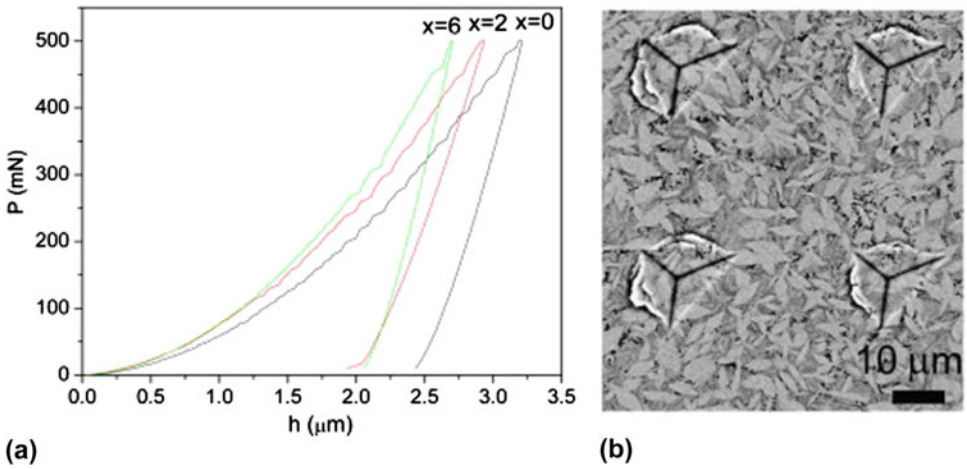

FIG. 8. (a) (*P–h*) nanoindentation curves of $Mg_{72-x}Zn_{23}Ca_5Pdx$ (x = 0, 2 and 6) alloys and (b) backscattered SEM image showing some indents made close to the center of the $Mg_{70}Zn_{23}Ca_5Pd_2$. (color online)

maximum hardness is attained by the $Al_{86}Ni_6Y_6Co_2$ alloy (i.e., 5.5 GPa), probably because of its amorphous state, but decreases sharply to 2.5 GPa with the addition of 0.5 at.% Pd. For this composition the value of E_r is also the lowest. Further addition of Pd to 1 at.% increases the hardness to 3 GPa. The composition with the largest $U_{plastic}/U_{total}$ corresponds to $Al_{86}Ni_6Y_{5.5}Co_2Pd_{0.5}$, corroborating its larger ability to store plastic energy during deformation.

Microalloying with Pd also has a large effect on the mechanical properties of alloys corresponding to the Mg–Zn–Ca–Pd system. The *P–h* nanoindentation curves with a maximum load of 500 mN are shown in Fig. 8(a). Some of the indentation impressions obtained at half the radius of the $Mg_{70}Zn_{23}Ca_5Pd_2$ rod are shown in Fig. 8(b). These indentation marks are large enough to embrace all the existing crystalline phases, thus the mechanical properties obtained are representative of the average behavior of the composite. The addition of 2 at.% Pd increases the hardness from 2.71 GPa ($x = 0$) to 3.56 GPa ($x = 2$). The hardness increase is mainly attributed to the lack of free volume in the crystalline alloy ($x = 2$) compared to the mainly amorphous one (for $x = 0$). The hardness further increases for $x = 6$, up to 3.90 GPa, which is consistent with the decrease of the maximum indentation depth from 2.905 μm (for $x = 2$) to 2.673 μm (for $x = 6$). This behavior could be mainly attributed to the presence of MgZn and Mg_6Pd. Hardness is usually regarded to be an important property for evaluating wear resistance but some authors have shown that the wear resistance can be better estimated from the H/E_r ratio.[68] Another parameter related to the wear performance is the resistance to plastic deformation,[69] which is proportional to H^3/E_r^2.

For Al-based alloys, the small addition of Pd[52] has a large influence on the microstructure and mechanical performance of Mg-based alloys. This behavior could be partly attributed to the low glass forming ability of alloys corresponding to these systems, which implies that small compositional change, such as microalloying would turn the microstructure from amorphous to crystalline. This work shows the usefulness to work with samples of dimensions close to the critical amorphous diameter so that microalloying could be more effective by turning the material from amorphous to partly or fully crystalline.

III. CONCLUSIONS

Previous discoveries have shown that microalloying technology is beneficial to tune the GFA and properties including mechanical, chemical, and physical properties of BMGs and BMG composites. From this review paper the following conclusions and tentative outlook have been presented:

(1) Studies about minor co-addition of alloying elements and their potential synergistic effects to produce BMGs with an excellent performance have been mainly overlooked in the past.

The chances of finding a composition with outstanding properties increase with the number of elements added but the analysis becomes more complex, which can be a limiting factor for the development on novel alloys through microalloying. To deal with such volume of information, the use of models can be very helpful. For example, a simplified thermodynamic model is proved to be useful to predict the change in GFA when two elements were co-added.[28] However, new models will be required in the future to handle the complexity of multiple element co-addition.

(2) Traditionally, microalloying has been used to tune the properties of crystalline or amorphous materials. For BMG composites, it has been recently shown that microalloying not only can be used to tune the properties of the amorphous matrix (i.e., changing the atomic short-range order, promoting the formation of clusters, etc.) but also can be used to tune the mechanical properties of the dispersed crystalline phase (i.e., the twinning propensity). It would be of interest to explore the possibility of multiple element co-addition to tune the properties of the amorphous phase with various microelements and the crystalline phase with others.

(3) Fabrication of BMGs with sizes close to the critical amorphous diameter is of interest for their application in industrial products. It also makes microalloying more effective to control the mechanical properties of BMGs since a small element addition can easily turn an amorphous material into a crystalline material upon cooling thus changing dramatically the mechanical behavior. Although it is currently possible to control the formation of crystalline phases in the amorphous matrix through proper microalloying, an accurate control is challenging mainly due to the high compositional sensitivity. Moreover, the chemical heterogeneity and variation in concentration of impurities across the parent sample might be of the same order as differences in the concentration of minor element/s added. One of the obstacles to be surmounted is the relatively low resolution of fast and cost-effective techniques to check alloy compositions, such as microanalysis in scanning electron microscope. This issue should be tackled to make the most of the microalloying technology.

REFERENCES

1. Z.P. Lu and C.T. Liu: Role of minor alloying additions in formation of bulk metallic glasses: A review. *J. Mater. Sci.* **39**, 3965 (2004).
2. L. Jiang, J.K. Li, P.M. Cheng, G. Liu, R.H. Wang, B.A. Chen, J.Y. Zhang, J. Sun, M.X. Yang, and G. Yang: Microalloying ultrafine grained Al alloy with enhanced ductility. *Sci. Rep.* **4**, 3605 (2013).
3. E.M. Carvalho and I.R. Harris: Constitutional and structural studies of the intermetallic phase, ZrCu. *J. Mater. Sci.* **15**, 1224 (1980).
4. Y.N. Koval, G.S. Firstov, and A.V. Kotko: Martensitic transformation and shape memory effect in ZrCu intermetallic compound. *Scr. Metall. Mater.* **27**, 1611 (1992).
5. D.B. Miracle: A structural model for metallic glasses. *Nat. Mater.* **3**, 697 (2004).
6. H.W. Sheng, W.K. Luo, F.M. Alamgir, J.M. Bai, and E. Ma: Atomic packing and short-to-medium-range order in metallic glasses. *Nature* **439**, 419 (2006).
7. A. Hirata, P. Guan, T. Fujita, Y. Hirotsu, A. Inoue, A.R. Yavari, T. Sakurai, and M. Chen: Direct observation of local atomic order in a metallic glass. *Nat. Mater.* **10**, 28 (2011).
8. W. Klement, Jr., R.H. Willens, and P. Duwez: Non-crystalline structure in solidified gold-silicon alloys. *Nature* **187**, 869 (1960).
9. D. Turnbull: Under what conditions can a glass be formed? *Comtemp. Phys.* **10**, 473 (1969).
10. D.E. Laughin and K. Hono: *Physical Metallurgy: 3-Volume Set*, 5th ed. (Elsevier, 2014).
11. Z.P. Lu and C.T. Liu: A new glass-forming ability criterion for bulk metallic glasses. *Acta Mater.* **50**, 3502 (2002).
12. Y. Wang, C.H. Shek, J. Qiang, C.H. Wong, Q. Wang, X. Zhang, and C. Dong: The e/a criterion for the largest glass-forming abilities of the Zr-Al-Ni(Co) alloys. *Mater. Trans.* **45**, 1180 (2004).
13. W. Jiao, D.Q. Zhao, D.W. Ding, H. Bai, and W.H. Wang: Effect of free electron concentration on glass-forming ability of Ca–Mg–Cu system. *J. Non-Cryst. Solids* **358**, 711 (2012).
14. J.J. Oak, D.V. Louzguine-Luzgin, and A. Inoue: Synthetic relationship between titanium and alloying elements in designing Ni-free Ti-based bulk metallic glass alloys. *Appl. Phys. Lett.* **91**, 053106 (2007).
15. F. Spaepen: A microscopic mechanism for steady state inhomogeneous flow in metallic glasses. *Acta Metall.* **25**, 407 (1977).
16. A.S. Argon: Plastic deformation in metallic glasses. *Acta Metall* **27**, 47 (1979).
17. F. Spaepen: Homogeneous flow of metallic glasses: A free volume perspective. *Scr. Mater.* **54**, 363 (2006).
18. A.L. Greer, Y.Q. Cheng, and E. Ma: Shear bands in metallic glasses. *Mater. Sci. Eng., R* **74**, 71 (2013).

19. K.K. Song, S. Pauly, Y. Zhang, P. Gargarella, R. Li, N.S. Barekar, U. Kühn, M. Stoica, and J. Eckert: Strategy for pinpointing the formation of B2 CuZr in metastable CuZr-based shape memory alloys. *Acta Mater.* **59**, 6620 (2011).
20. S. Pauly, J. Das, J. Bednarcik, N. Mattern, K.B. Kim, D.H. Kim, and J. Eckert: Deformation-induced martensitic transformation in Cu-Zr-(Al,Ti) bulk metallic glass composites. *Scr. Mater.* **60**, 431 (2009).
21. Y. Wu, D.Q. Zhou, W.L. Song, H. Wang, Z.Y. Zhang, D. Ma, X.L. Wang, and Z.P. Lu: Ductilizing bulk metallic glass composite by tailoring stacking fault energy. *Phys. Rev. Lett.* **109**, 245506 (2012).
22. E. Ma, Y.M. Wang, Q.H. Lu, M.L. Sui, L. Lu, and K. Lu: Strain hardening and large tensile elongation in ultrahigh-strength nano-twinned copper. *Appl. Phys. Lett.* **85**, 4932 (2004).
23. K. Lu, L. Lu, and S. Suresh: Strengthening materials by engineering coherent internal boundaries at the nanoscale. *Science* **324**, 349 (2009).
24. O. Gendelman, A. Joy, P. Mishra, I. Procaccia, and K. Samwer: On the effect of microalloying on the mechanical properties of metallic glasses. *Acta Mater.* **63**, 209 (2014).
25. D.H. Xu, G. Duan, and W.L. Johnson: Unusual glass-forming ability of bulk amorphous alloys based on ordinary metal copper. *Phys. Rev. Lett.* **92**, 245504 (2004).
26. Y. Zhang, J. Chen, G.L. Chen, and X.J. Liu: Glass formation mechanism of minor yttrium addition in CuZrAl alloys. *Appl. Phys. Lett.* **89**, 131904 (2006).
27. Q. Wang, C.T. Liu, Y. Yang, J.B. Liu, Y.D. Dong, and J. Lu: The atomic-scale mechanism for the enhanced glass-forming-ability of a Cu-Zr based bulk metallic glass with minor element additions. *Sci. Rep.* **4**, 4648 (2014).
28. R. Li, S.J. Pang, M.C. Ma, and T. Zhang: Influence of similar atom substitution on glass formation in (La-Ce)-Al-Co bulk metallic glasses. *Acta Mater.* **55**, 3719 (2007).
29. C.T. Liu, M.F. Chisholm, and M.K. Miller: Oxygen impurity and microalloying effect in a Zr-based bulk metallic glass alloy. *Intermetallics* **10**, 1105 (2002).
30. G.J. Fan, L.F. Fu, D.C. Qiao, H. Choo, P.K. Liaw, N.D. Browning, and J.F. Löffler: Effect of microalloying on the glass-forming ability of $Cu_{60}Zr_{30}Ti_{10}$ bulk metallic glass. *J. Non-Cryst. Solids* **353**, 4218 (2007).
31. S. González, I.A. Figueroa, H. Zhao, H.A. Davies, I. Todd, and P. Adeva: Effect of mischmetal substitution on the glass-forming ability of Mg–Ni–La bulk metallic glasses. *Intermetallics* **17**, 968 (2009).
32. B. Zberg, P.J. Uggowitzer, and J.F. Löffler: MgZnCa glasses without clinically observable hydrogen evolution for biodegradable implants. *Nat. Mater.* **8**, 887 (2009).
33. D.V. Louzguine-Luzgin and A. Inoue: Structure and transformation behaviour of a rapidly solidified Al–Y–Ni–Co–Pd alloy. *J. Alloys Compd.* **399**, 78 (2005).
34. P. Yu, H.Y. Bai, and W.H. Wang: Superior glass-forming ability of CuZr alloys from minor additions. *J. Mater. Res.* **21**, 1674 (2006).
35. Z.P. Lu, H. Bei, and C.T. Liu: Recent progress in quantifying glass forming ability of metallic glasses. *Intermetallics* **17**, 618 (2007).
36. A. Takeuchi and A. Inoue: Classification of bulk metallic glasses by atomic size difference, heat of mixing and period of constituent elements and its application to characterization of the main alloying element. *Mater. Trans.* **46**, 2817 (2005).
37. J.C. Slater: Atomic radii in crystals. *J. Chem. Phys.* **41**, 3199 (1964).
38. www.chemicool.com.
39. S. González, I.A. Figueroa, and I. Todd: Influence of minor alloying additions on the glass-forming ability of Mg–Ni–La bulk metallic glasses. *J. Alloys Compd.* **484**, 612 (2009).
40. P. Pérez, S. González, G. Garcés, and P. Adeva: Influence of mischmetal composition on crystallization and mechanical properties of Mg_{80}-Ni_{10}-MM_{10} alloys. *Intermetallics* **17**, 504 (2009).
41. Y. Cheng, E. Ma, and H. Sheng: Atomic level structure in multicomponent bulk metallic glass. *Phys. Rev. Lett.* **102**, 245501 (2009).
42. K.S. Bondi, A.K. Gangopadhyay, Z. Marine, T.H. Kim, A. Mukhopadhyay, A.I. Goldman, W.E. Buhro, and K.F. Kelton: Effects of microalloying with 3d transition metals on glass formation in AlYFe alloys. *J. Non-Cryst. Solids* **353**, 4723 (2007).
43. B. Zhang, D.Q. Zhao, M.X. Pan, R.J. Wang, and W.H. Wang: Formation of cerium-based bulk metallic glasses. *Acta Mater.* **54**, 3025 (2006).
44. S.M. Chathoth, B. Damaschke, J.P. Embs, and K. Samwer: Giant changes in atomic dynamics on microalloying metallic melt. *Appl. Phys. Lett.* **95**, 191907 (2007).
45. F. Qin, H. Zhang, A. Wang, B. Ding, and Z. Hu: Effect of Pd on GFA and thermal stability of Zr-based bulk amorphous alloy. *J. Mater. Sci. Technol.* **20**, 160 (2004).
46. S. González, P. Pérez, E. Rossinyol, S. Suriñach, M.D. Baró, E. Pellicer, and J. Sort: Drastic influence of minor Fe or Co additions on the glass forming ability, martensitic transformations and mechanical properties of shape memory Zr–Cu–Al bulk metallic glass composites. *Sci. Technol. Adv. Mater.* **15**, 035015 (2014).
47. F.A. Javid, N. Mattern, S. Pauly, and J. Eckert: Effect of cobalt on phase formation, microstructure, and mechanical properties of $Cu_{(50-x)}Co_xZr_{50}$ (x = 2, 5, 10, 20 at.%) alloys. *Metall. Mater. Trans. A* **43 A**, 2631 (2012).
48. F.A. Javid, N. Mattern, M. Samadi Khoshkhoo, M. Stoica, S. Pauly, and J. Eckert: Phase formation of $Cu_{(50-x)}Co_xZr_{50}$ (x = 0–20 at.%) alloys: Influence of cooling rate. *J. Alloys Compd.* **590**, 428 (2014).
49. Y. Wang, J. Wang, and C. Li: Effect of Si, Pd, and La additions on glass forming ability and thermal stability of Zr–Ni-based amorphous alloys. *J. Alloys Compd.* **509**, 3262 (2011).
50. J.K. Lee, W.T. Kim, and D.H. Kim: Effects of Pd addition on the glass forming ability and crystallization behavior in the Ni–Zr–Ti alloys. *Mater. Lett.* **57**, 1514 (2003).
51. A. Inoue: Stabilization of metallic supercooled liquid and bulk amorphous alloys. *Acta Mater.* **48**, 279 (2000).
52. S. González, J. Sort, D.V. Louzguine-Luzgin, J.H. Perepezko, M.D. Baró, and A. Inoue: Tuning the microstructure and mechanical properties of Al-based amorphous/crystalline composites by addition of Pd. *Intermetallics* **18**, 2377 (2010).
53. S. González, E. Pellicer, J. Fornell, A. Blanquer, L. Barrios, E. Ibañez, P. Solsona, S. Suriñach, M.D. Baró, C. Nogués, and J. Sort: Improved mechanical performance and delayed corrosion phenomena in biodegradable Mg-Zn-Ca alloys through Pd-alloying. *J. Mech. Behav. Biomed. Mater.* **6**, 53 (2012).
54. S-i. Yamaura, H. Kimura, and A. Inoue: Structure and properties of melt-spun Mg–Pd binary alloys. *Mater. Trans.* **44**, 1895 (2003).
55. F.R. Boer, R. Boom, W.C.M. Matterns, A.R. Miedema, and A.K. Niessen: *Cohesion in Metals* (North-Holland, Amsterdam, 1988).
56. G.R. Garret, M.D. Demetriou, J. Chen, and W.L. Johnson: Effect of microalloying on the toughness of metallic glasses. *Appl. Phys. Lett.* **101**, 241913 (2012).
57. Q. He, Y-Q. Cheng, E. Ma, and J. Xu: Locating bulk metallic glasses with high fracture toughness: Chemical effects and composition optimization. *Acta Mater.* **59**, 202 (2011).
58. G.B. Bokas, G.A. Evangelakis, and Ch.E. Lekka: Modifications of $Cu_xZr_{12-x}Y$ icosahedra upon ($0 < x < 12$ Y = Be, Mg, Al, Si, P, Nb, Ag) substitutions by density functional theory computations. *Comput. Mater. Sci.* **50**, 2658 (2011).

59. K. Georgarakis, A.R. Yavari, D.V. Louzguine-Luzgin, J. Antowicz, M. Stoica, Y. Li, M. Satta, A. LeMoulec, G. Vaugham, and A. Inoue: Atomic structure of Zr-Cu glassy alloys and detection of deviations from ideal solution behaviour with Al addition by x-ray diffraction using synchrotron light in transmission. *Appl. Phys. Lett.* **94**, 191912 (2009).
60. C.P. Kim, J-Y. Suh, A. West, M.L. Lind, R. Dale Conner, and W.L. Johnson: Fracture toughness study of new Zr-based Be-bearing bulk metallic glass. *Scr. Mater.* **60**, 80 (2009).
61. Q. Hu, M.W. Fu, and X.R. Zeng: Thermostability and thermoplastic formability of $(Zr_{65}Cu_{17.5}Ni_{10}Al_{7.5})_{100-x}RE_x$ (x = 0.25–3.25, RE: Y, Gd, Tb, Dy, Ho, Er, Tm, Yb, Lu) bulk metallic glasses. *Mater. Des.* **64**, 301 (2014).
62. J. Wang, Y. Li, S. Huang, Y. Wei, X. Xi, K. Cai, and F. Pan: Effects of Y on the microstructure, mechanical and bio-corrosion properties of MgZnCa bulk metallic glass. *J. Mater. Sci. Technol.* **30**, 1255 (2014).
63. X. Hong-wei, D. Yu-lei, and D. Yu: Effects of Y addition on structural and mechanical properties of CuZrAl bulk metallic glass. *Trans. Nonferrous Met. Soc. China* **22**, 842 (2012).
64. X.P. Nie, X.M. Xu, Q.K. Jiang, L.Y. Chen, Y. Xu, Y.Z. Fang, G.Q. Xie, M.F. Luo, F.M. Wu, X.D. Wang, Q.P. Cao, and J.Z. Jiang: Effect of microalloying of Nb on corrosion resistance and thermal stability of ZrCu-based bulk metallic glasses. *J. Non-Cryst. Solids* **355**, 203 (2009).
65. S. Pauly, S. Gorantla, G. Wang, U. Kühn, and J. Eckert: Transformation-mediated ductility in CuZr-based bulk metallic glasses. *J. Nat. Mater.* **9**, 473 (2010).
66. S.W. Seo and D. Schryvers: TEM investigation of the microstructure and defects of CuZr martensite. Part I: Morphology and twin systems. *Acta Mater.* **46**, 1165 (1998).
67. J. Sort, A. Zhilyaev, M. Zielinska, J. Nogués, S. Suriñach, T. Thibault, and M.D. Baró: Microstructural effects and large microhardness in cobalt processed by pressure torsión consolidation of ball milled powders. *Acta Mater.* **51**, 6385 (2003).
68. T.L. Oberle: Properties influencing wear of metals. *J. Met.* **3**, 438 (1951).
69. T.Y. Tsui, G.M. Pharr, W.C. Oliver, C.S. Bhatia, R.L. White, S. Anders, A. Anders, and I.G. Brown: Nanoindentation and nanoscratching of hard coatings for magnetic disks. *Mater. Res. Soc. Symp. Proc.* **383**, 447 (1995).